



LAWRENCE  
LIVERMORE  
NATIONAL  
LABORATORY

# Differential Synthetic Aperture Ladar

E. A. Stappaerts, E.T. Scharlemann

February 25, 2005

Differential Synthetic Aperture Ladar

## **Disclaimer**

---

This document was prepared as an account of work sponsored by an agency of the United States Government. Neither the United States Government nor the University of California nor any of their employees, makes any warranty, express or implied, or assumes any legal liability or responsibility for the accuracy, completeness, or usefulness of any information, apparatus, product, or process disclosed, or represents that its use would not infringe privately owned rights. Reference herein to any specific commercial product, process, or service by trade name, trademark, manufacturer, or otherwise, does not necessarily constitute or imply its endorsement, recommendation, or favoring by the United States Government or the University of California. The views and opinions of authors expressed herein do not necessarily state or reflect those of the United States Government or the University of California, and shall not be used for advertising or product endorsement purposes.

## Differential Synthetic Aperture Ladar

Eddy A. Stappaerts and E.T. Scharlemann  
Lawrence Livermore National Laboratory

January 2005

We report a differential synthetic aperture ladar (DSAL) concept that relaxes platform and laser requirements compared to conventional SAL. Line-of-sight translation/vibration constraints are reduced by several orders of magnitude, while laser frequency stability is typically relaxed by an order of magnitude. The technique is most advantageous for shorter laser wavelengths, ultraviolet to mid-infrared. Analytical and modeling results, including the effect of speckle and atmospheric turbulence, are presented.

Synthetic aperture ladars are of growing interest, and several theoretical<sup>1,2</sup> and experimental<sup>3-5</sup> papers have been published on the subject. Compared to RF synthetic aperture radar (SAR), platform/ladar motion and transmitter bandwidth constraints are especially demanding at optical wavelengths. For mid-IR and shorter wavelengths, deviations from a linear trajectory along the synthetic aperture length have to be sub-micron, or their magnitude must be measured to that precision for compensation. The laser coherence time has to be the synthetic aperture transit time, or transmitter phase has to be recorded and a correction applied on detection.

The DSAL concept\* is depicted in Fig. 1 for a “Stripmap mode”<sup>6</sup> configuration. The transceiver aperture, of width  $d$ , is divided into two equal subapertures along the flight direction. The laser beam is transmitted through the full aperture, while return radiation is collected through both subapertures. Phase differentials between the subapertures are measured by heterodyning with a common local oscillator. These steps are repeated every distance  $d/4$  of travel.

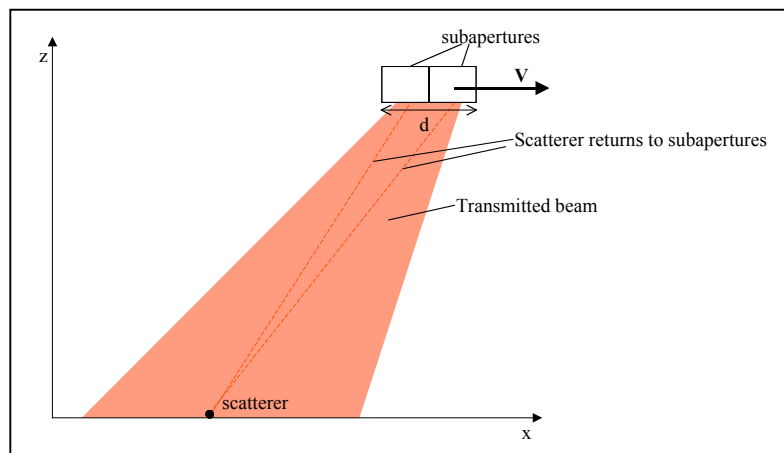


Fig. 1. DSAL Concept

As will be shown below, the phase in either subaperture can be reconstructed by summing these differentials. In the process, common-mode phase errors between the two subapertures cancel. In particular, DSAL is insensitive to line-of-sight translation and vibration. As an example, for a single point source scatterer at location  $x_p$ , the path length difference to the center of the two subapertures is:

$$\Delta s(z) \sim \frac{(x - x_p + d/4) - (x - x_p - d/4)}{2z} \sim \frac{(x - x_p)}{2z}$$

and, to first order in  $z$ :

$$\delta(\Delta\phi) = \frac{\delta z}{z} \Delta\phi$$

Since  $\Delta\phi$  is on the order of  $2\pi$ , the error is negligible for realistic  $\delta z$  values. Laser coherence is only required over a single roundtrip since differential phase measurements are independent. Phase distortions in the laser and local oscillator waveforms are common-mode as well, but such distortions must still need to be kept small, or recorded for maximum range resolution (not discussed in the present paper). Pointing stability requirements are similar to SAL.

The ideal, noise-free operation described above is degraded by detection noise, in particular inherent LO shot-noise. Since this noise is uncorrelated for the two differential measurements from which absolute phases are computed, an SNR-dependent stitching error results that accumulates along the synthetic aperture, in a random walk type manner. However, at optical wavelengths, unlike RF, the number of samples along a synthetic aperture length,  $N_s \sim 4\lambda d/R^2$ , is small, and the image distortion is modest.

We now present a more quantitative discussion of the DSAL concept. Equations 1 describe the received field in the two subapertures, for a Gaussian transmitter beam. Simulations have shown the conclusions derived from them to be generally correct.

Right subaperture:

$$Er_j = \sum_p a_p e^{-\frac{(x_j - x_p)^2}{w_0^2}} e^{-\frac{ik(x_j - x_p)}{2R}} e^{-\frac{ik(x_j + d/4 - x_p)}{2z}}$$

Left subaperture:

$$El_j = \sum_p a_p e^{-\frac{(x_j - x_p)^2}{w_0^2}} e^{-\frac{ik(x_j - x_p)}{2R}} e^{-\frac{ik(x_j - d/4 - x_p)}{2z}}$$

where  $x_j = j*d/4$  and  $x_p$  are the positions of the aperture center and target point scatterers, respectively,  $z$  is the range, and  $w_0$  and  $R(z)$  are the transmitter beam waist and radius of curvature at range  $z$ , respectively. It can be verified by inspection that, for  $R=z$ ,  $E_{j+1}=E_r_j$ , i.e. the field in the left subaperture for sample  $(j+1)$  equals the field in the right subaperture for sample  $j$ . Therefore, absolute phases can be obtained by adding these differentials, as illustrated in Fig. 2. The condition  $R=z$  means that the object must be in the far field of the transmitter, which is typically the case; simulations show that deviations up to approximately 10% are acceptable (intermediate field).

Platform Position	Measured Phase Differential	Calculated Phase
		$\phi_1=0$
I	$\phi_2-\phi_1$	$\phi_2$
II	$\phi_3-\phi_2$	$\phi_3$
III	$\phi_4-\phi_3$	$\phi_4$

Fig.2. Differential and absolute phases versus platform position

Images are constructed from the subaperture fields using Eq. 2, adapted from the conventional SAR theory <sup>6</sup>:

$$I_m = \left| \sum_j E_{r_j} e^{-i\phi_{r_j}} G_{j+m} \right|^2$$

where:

$$G_j = e^{\frac{ikx_j^2}{2R}} e^{\frac{ik(x_j+d/4)}{2L}}$$

Figures 3-4 show representative wave-optics simulation results. Shot noise was added, for each phase measurement, using Poisson statistics for the received photon number. The associated phase error variance can be shown to be  $\sigma^2(\delta\phi)=1/n_s$ , where  $n_s$  is the number of photo-electrons. Figure 3 shows images for an ideal straight trajectory, for  $n_s=8$ ; even for small photon numbers, SAL and DSAL provide similar performance. Figure 4 illustrates how DSAL operation is insensitive to LOS motion/vibration when SAL images are not feasible; a random phase according to a uniform probability density function was added at each platform position.

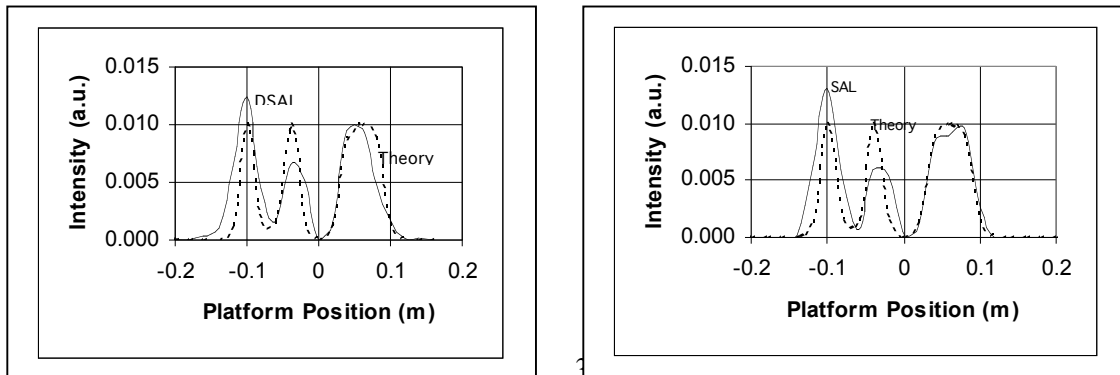


Fig.3. Reconstructed images with shot noise,  $n_s=8$ . The dotted lines are the ideal images.  
Left: DSAL, Right: SAL

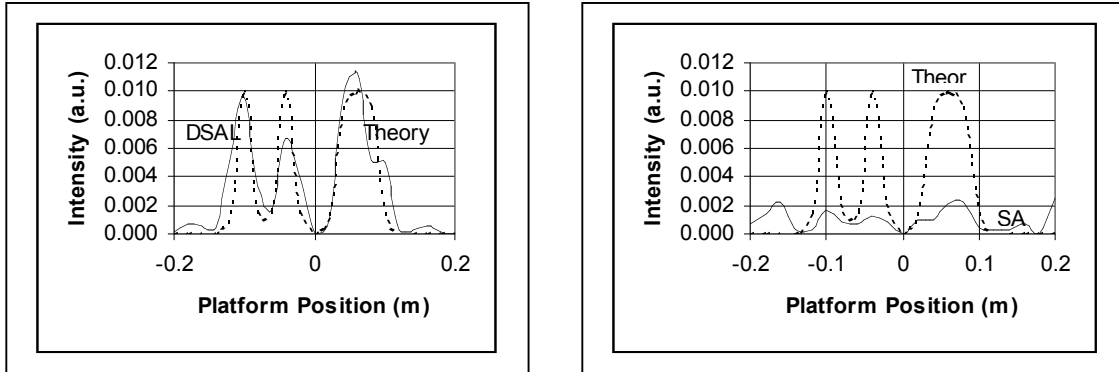


Fig.4. Reconstructed images with random vibration ( $\lambda/5$ ) + shot noise,  $n_s=8$ .  
Left: DSAL, Right: SAL

Preliminary studies have been performed on the effect of speckle and atmospheric turbulence. They show that both effects are similar for DSAL and SAL. Figure 5 shows 3D simulation results for two targets, for two values of the Fried parameter,  $r_0$ , for noise-free detection: SAL and DSAL results are indistinguishable. Significant image degradation is observed, for both configurations, for the smaller  $r_0$  value.

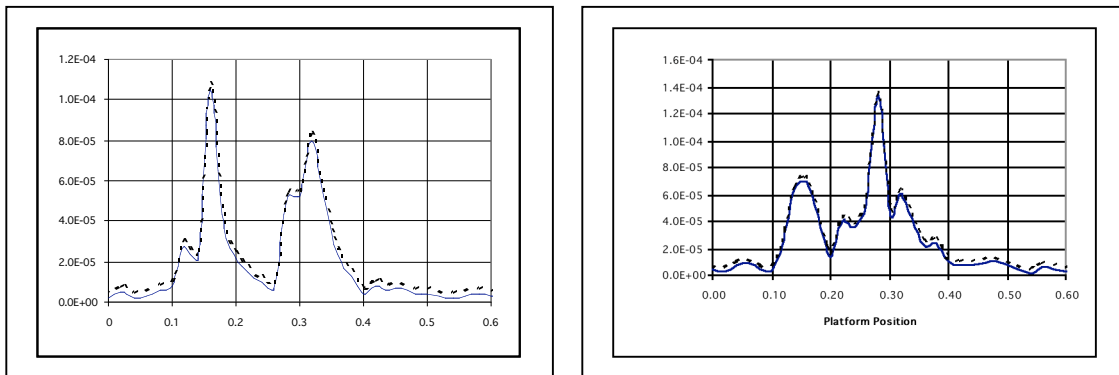


Fig.5. Imaging through turbulence:  $\lambda=2 \mu\text{m}$ ,  $d = 8 \text{ cm}$ , range = 13.3 km . Left:  $r_0(\text{up}) = 1 \text{ m}$ , right:  $r_0(\text{up}) = 3.5 \text{ cm}$ . A small vertical offset was added to the dashed SAL images.

In conclusion, analytical and modeling studies have been carried out on a differential synthetic aperture ladar concept. The concept greatly relaxes motion/vibration and laser spectral purity requirements, and is most beneficial for shorter wavelength, UV-to-MIR, imaging systems.

References

1. D. Park and J.H. Shapiro, "Performance analysis of optical synthetic aperture radars", Laser Radar III, Proc. SPIE 999, 100-116 (1998)
  2. T.J. Karr, "Resolution of synthetic aperture imaging through turbulence", JOSA A, Vol. 20, No. 6, 1067-1083, (2003)
  3. T.J. Green, Fr., S. Marcus and B. D. Colella, "Synthetic aperture-radar imaging with a solid-state laser", Applied Optics 34, 6941-6949 (1995)
  4. C.C. Aleksoff, J.S. Accetta, L.M. Peterson, A.M. Tai, A. Klooster, K.S. Schroeder, R.M. Majewski, J.O. Abshier, and M. Fee, "Synthetic aperture imaging with a pulsed CO<sub>2</sub> TEA laser, Proc. SPIE 783, 29-40, (1987)
  5. S. Yoshikada and T. Aruga, "Short-range verification experiment of a trial one-dimensional synthetic aperture infrared laser operated in the 10  $\mu$ m band", Applied Optics 39, 1421-1425 (2000)
  6. Donald R. Wehner, "High Resolution Radar, Chapter 6, Artech House, 1987
  7. D.L. Fried, "optical resolution through a randomly inhomogeneous medium for very long and very short exposures", JOSA Vol. 56 No. 10, 1372-1379 (1966)
- U.S. Patent Serial Number 10/402053.

This work was performed under the auspices of the U. S. Department of Energy by the University of California, Lawrence Livermore National Laboratory under Contract No. W-7405-Eng-48.